Innovative Infrastructure Solutions (2024) 9:130
https://doi.org/10.1007/s41062-024-01446-0

PRACTICE-ORIENTED PAPER

Assessing the geotechnical properties of peridotite rocks in dry and saturated conditions

K. Diamantis[1] · R. Khajevand[2] · D. Fereidooni[2]

Received: 8 June 2023 / Accepted: 15 March 2024 / Published online: 4 April 2024

Abstract
The main objective of this research is to assess the effect of water saturation on the physical, dynamic and mechanical properties of peridotite rocks. For this purpose, 35 samples of peridotite rocks, taken from central Greece, were tested and the static and dynamic test results were determined in saturated condition. Also, dynamic elastic constants were calculated from wave velocity. Based on the results of unit weight, P-wave velocity and uniaxial compressive strength of the studied rocks, they were classified from very high to extremely strong. A comparative study between the obtained results and saturated properties from previous studies was conducted. The dynamic tests showed the P- and S-wave velocities increased averagely 4.61 and 5.01%, respectively, after saturation. According to the mechanical tests, UCS, E, and BTS are averagely decreased 8.19, 8.43 and 11.71%, respectively, after saturation. Moreover, regression analyses were applied to define the relations between the properties of the rocks in the two mentioned conditions. All the correlations between the properties are linear or logarithmic and the coefficient of determination (R^2) ranges between 0.55 and 1. The obtained results revealed changes in the physical, dynamic and mechanical properties in the presence of water.

Keywords Strength · Deformation · Peridotite · Dry and saturated conditions · Coefficient of determination

Introduction

Uniaxial Compressive Strength (UCS), tensile strength (TS) and the elasticity modulus (E) are important geotechnical parameters widely used in rock engineering projects [1, 2]. A large number of geotechnical hazards such as landslides [3], pillar instability [4], fault activation [5] and ground subsidence [6] are related to water-rock interaction effects, as the presence of water significantly reduces rock strength and stiffness. Therefore, a comprehensive and in-depth knowledge of water-rock interaction effects on rock properties is crucial for preventing and solving problems related to rock mechanics applications.

Many works have studied the relations between dry and saturated uniaxial compressive strength for different rocks [7–17]. The influence of water content on the tri-axial compressive strength, elastic modulus, tensile strength, shear strength and fracture toughness has been reported by several researchers [18–21]. All of them revealed that presence of water reduces strength and deformations of different rocks. This reduction is due to variation in mineralogy, texture and lithology in different rock types.

Determining strength and deformation of rocks by direct and destructive tests requires core specimens with high quality, partly expensive, difficult operation and considerable time, while in indirect methods, these specifications are not necessary [22–25]. Different studies proposed empirical equations and developed experimental models for indirect estimation of strength and deformation parameters of rocks in dry and saturated conditions. Although many studies have attempted to describe the effect of water on the mechanical properties, no one has been focused on peridotites. But, due to the fact that peridotites have become important earth crust components in some areas like south-eastern Europe,

✉ K. Diamantis
kostasdiam@geol.uoa.gr

R. Khajevand
r.khajevand@std.du.ac.ir

D. Fereidooni
d.fereidooni@du.ac.ir

1 Department of Geology and Geoenvironment, School of Science, National and Kapodistrian University of Athens, University Campus, 15784 Zografou, Athens, Greece

2 School of Earth Sciences, Damghan University, Damghan, Semnan, Iran

especially in the countries of former Yugoslavia, Albania, Greece, Turkey etc., many studies should be focused on them. For this reason, within the framework of the present research, thirty five samples taken from central part of Greece are tested to determine the dynamic (Compressional, V_P and shear wave velocity V_S) and the mechanical (uniaxial compressive strength, UCS, elasticity modulus, E and Brazilian tensile strength, BTS) properties in saturated states. The same dynamic and mechanical characteristics from the same locations with dry conditions as well as physical properties in dry (dry unit weight, γ_{dry}) and saturated states (saturated unit weight, γ_{sat}) were performed by Diamantis [26, 27]. Both dry and saturated conditions were based on the recommended methods of International Society of Rock Mechanics (ISRM) and American Society for Testing and Materials (ASTM). The objective of this research is to assess the effect of saturation on strength and deformation of the peridotite rocks. In other words, understanding the effect of the water presence of on the quality of engineering materials is the most important goal pursued by this research. Thus, simple regression analyses were used for indirect estimating the strength and deformation of peridotite rocks through the physical and dynamic properties and some empirical equations were proposed between dry and saturated characteristics. The determination coefficients (R^2) and the equations of the fitted lines were calculated by the "least squares" method.

Materials and methods

The peridotites used for the experiments were retrieved from two regions of the central Greece. The first area is located at the eastern-southeastern parts of Kallidromo Mt. (near the villages of Kallidromo, Reginio and Modio, Fig. 1), while the second area is the western parts of Othrys Mt. (near the villages of Moschokarya, Makryrrachi and Domokos, Fig. 1). Basing on the field investigations, the peridotites are mainly medium-grained, homogeneous and isotropic belonging to the ophiolitic complex of Orthrys. According to Diamantis [26, 27], they present a granular or porphyritic structure, compact texture without preferred mineral orientation and they are dominantly formed by olivine, orthopyroxene (mainly enstatite) and chromite minerals belonging to the parent rocks. In fact these Peridotites have been influenced by serpentinization (i.e., low-temperature metamorphic process, [17, 28]) and the primary magnetic minerals transformed into secondary minerals. Serpentinization degree of the tested samples varies between 3 and 27% [26, 27].

The data pertains to peridotites samples from thirty-five sites in the above-mentioned study areas (from the surface). The test samples were cored from fresh intact rock blocks and were cut in cylindrical specimens (6 to 10 per sample). A diamond cutter with an acute blade and a grinder were used for the cutting and polishing operations respectively. The size, shape and ends of samples followed the ISRM [29] testing specifications. The height-to-diameter ratio of the test specimens was recommended to be between 2.0 and 2.5 and the diameter of the prepared cylindrical rock specimens ranged between 53 and 55 mm with the aim of reducing the uncertainty of the sample size on the measured properties and especially on strength. Firstly, the specimens were inspected macroscopically and only the homogeneous, isotropic, un-weathered (or slightly weathered), and free of visible joints, cracks, fissures, or other discontinuities, peridotites were considered.

Results and discussion

Physical properties

The physical properties including effective porosity (n_e), water absorption (W_a), dry unit weight (γ_{dry}) and saturated unit weight (γ_{sat}) were obtained by Diamantis [26, 27] for 35 samples of peridotite rocks according to ISRM [29] methods. The results of physical properties tests were calculated using the following equations.

$$n = \frac{V_v}{V_t} = \frac{(M_{\text{sat}} - M_s)/\rho_w}{(M_{\text{sat}} - M_{\text{sub}})/\rho_w} \times 100 \tag{1}$$

$$\gamma_{\text{dry}} = \frac{W_{\text{dry}}}{V_t} = \frac{M_s \times g}{(M_{\text{sat}} - M_{\text{sub}})/\rho_w} \tag{2}$$

$$\gamma_{\text{sat}} = \frac{W_{\text{sat}}}{V_t} = \frac{M_{\text{sat}} \times g}{(M_{\text{sat}} - M_{\text{sub}})/\rho_w} \tag{3}$$

$$W_a = \frac{M_{\text{sat}} - M_s}{M_s} \times 100 \tag{4}$$

where, V_v is the volume of the voids (m^3), V_t is the total volume of the specimen (m^3), M_{sat} is the saturated mass of the specimen (dry on the surface, g), $M_s$is the dry mass of the specimen (g), M_{sub} is the submerged mass of the specimen (g),W_{dry} is the dry weight of the specimen (kN/m^3), g is the gravitational acceleration (9.807 m/s^2), and ρ_w, is the density of water (1 g/cm^3).

The minimum, the maximum, the average value and the standard deviation of the physical properties are listed in Table 1. The effective porosity values range between 0.06 and 0.26%. The porosity of the studied rocks classified as vary low porosity based on [30] classifications. Average value of water absorption is equal to 0.05%. Average

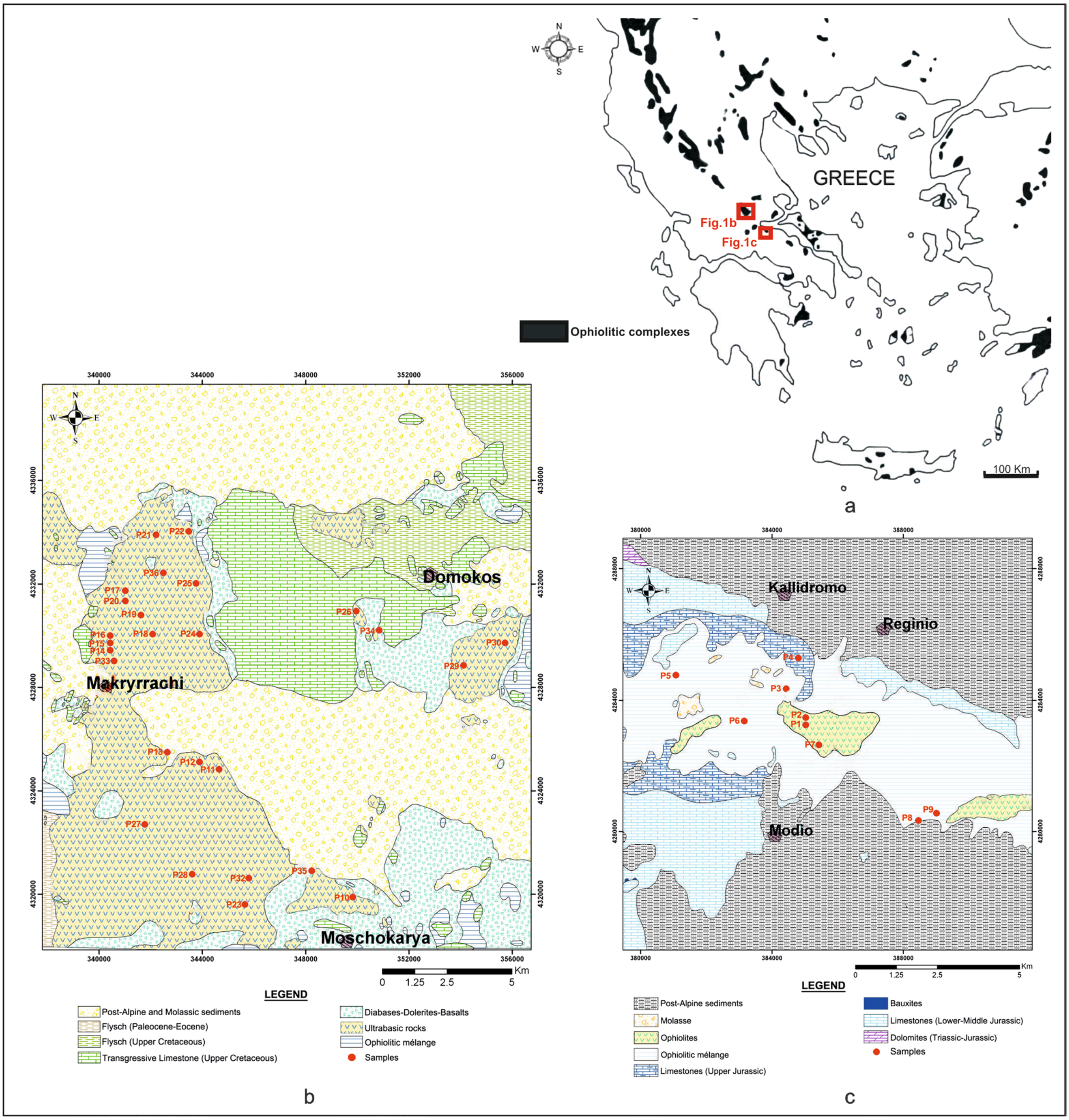

Fig. 1 **a** Study areas and ophiolitic complexes in Greece and neighboring countries. **b** Lithological map of the study area at Othrys Mt. **c** Lithological map of the study area at Kallidromo Mt. The exact locations of the samples collected are also displayed on both lithological maps (coordinates belong to the Greek Geodetic Reference System 1987: GGRS87)

Table 1 Basic descriptive statistical analysis of the physical properties for the peridotite rocks [26, 27]

Property	Minimum value	Maximum value	Mean value	Standard deviation
Effective porosity, n (%)	0.06	0.26	0.16	0.07
Water absorption, W_a (%)	0.02	0.08	0.05	0.02
Dry unit weight, γ_{dry} (kN/m^3)	30.64	33.33	32.10	0.88
Saturated unit weight, γ_{sat}(KN/m^3)	30.66	33.34	32.11	0.87

value of dry and saturated unit weight are obtained in range of 30.64–33.33 kN/m^3 and 30.66–33.34 kN/m^3, respectively. By unit weight point of view the studied samples are classified as very high according to IAEG [31] classification.

Correlations between physical properties were performed and graphs of regression analyses are shown in Fig. 2. Based on the results direct linear correlations ($y = ax + b$) with strong coefficient of determination ($R^2 = 1$ and 0.99) were obtained between dry and saturated unit weight and porosity and water absorption, respectively (Fig. 2a and b). Good reverse linear correlations with high coefficient of determination equal to $R^2 = 0.94$ and $R^2 = 0.95$ was found between dry unit weight and porosity, and saturated unit weight and water absorption, respectively (Fig. 2c and d). Therefore, when porosity and water absorption decrease the unit weight increases.

Ultrasonic wave velocity

Several works [23, 32–34] studied the relation between ultrasonic wave velocity and different characteristics of rocks and showed that rock properties are closely related to wave velocity. Especially, Kurtulus et al. [33] studied the relation between porosity and V_P in serpentinized ultrabasic rocks by simple regression analysis and presented experimental equation with coefficient of determination $R^2 = 0.87$.

In this research, ultrasonic wave velocity including primary or compressional wave (V_P) and secondary or shear wave (V_S) in saturated conditions were performed based on recommend methods of [35]. The prepared core specimens with diameter of 54 mm and a length to diameter ratio in range of 2–2.5 were used for determining P and S wave velocity of studied rocks. Also, V_p and V_s values in dry states obtained by Diamantis, [26, 27] were used in order to be compared with saturated values. The P-wave velocity values ranged from 7048 to 7981 m/s and 7591 to 8174 m/s in dry and saturated conditions, respectively (Table 2). Therefore,

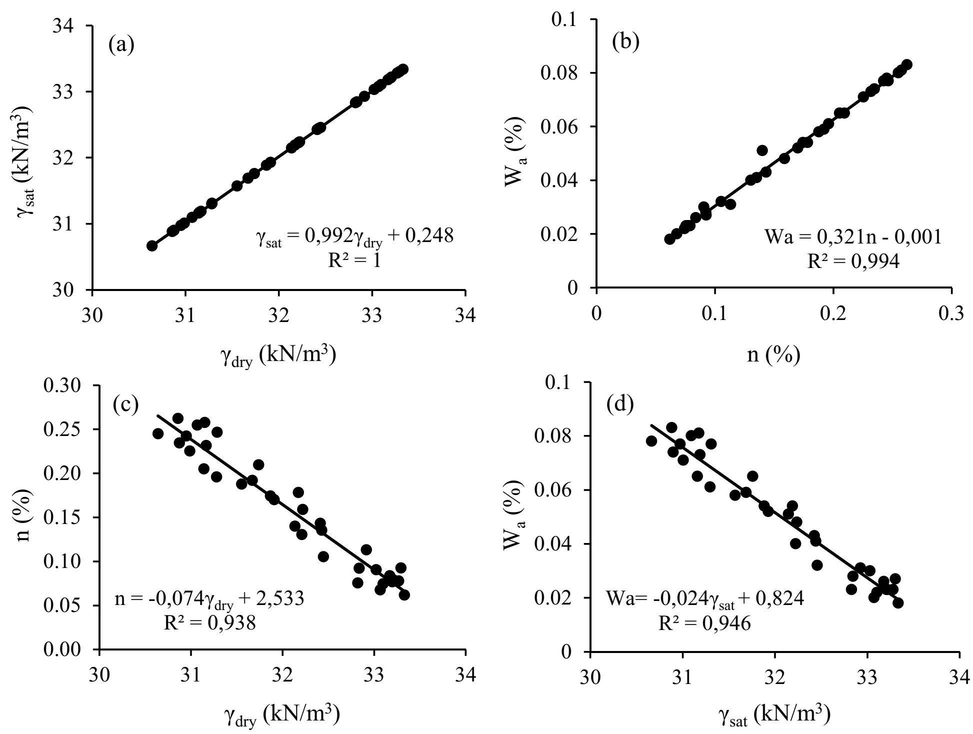

Fig. 2 Correlations between **a** dry unit weight and saturated unit weight, **b** porosity and water absorption, **c** dry unit weight and porosity and **d** saturated unit weight and water absorption

Table 2 Basic descriptive statistical analysis of the ultrasonic wave velocity for the peridotite rocks

Property	Minimum value	Maximum value	Mean value	Standard deviation
Dry primary wave velocity, $V_{P(\text{dry})}$ (m/s)	7048	7981	7553	301.64
Saturated primary wave velocity, $V_{P(\text{sat})}$ (m/s)	7591	8174	7895	180.46
Dry secondary wave velocity, $V_{S(\text{dry})}$ (m/s)	3816	4560	4212	227.96
Saturated secondary wave velocity, $V_{S(\text{sat})}$ (m/s)	4111	4733	4420	189.96

the P-wave velocity averagely 4.61% increased after saturation. According to IAEG [31] rock classification, the P-wave velocity values classified as very high. The S-wave velocity values were in range of 3816–4560 m/s and 4111–4733 m/s, in dry and saturated conditions, respectively (Table 2). So, the S-wave velocity averagely 5.01% increased after saturation. The minimum, the maximum, the average value and the standard deviation of the ultrasonic wave velocities are listed in Table 2.

Correlations between porosity and dry and saturated P-wave velocities are presented in Fig. 3a. As can be seen, reverse logarithmic relations were found between the porosity and P-wave velocity with coefficient of determination $R^2=0.86$ and $R^2=0.77$ for dry and saturated conditions, respectively. Correlations between porosity and dry and saturated S-wave velocity as reverse logarithmic relations with coefficient of determination equal to $R^2=0.88$ and $R^2=0.87$ for dry and saturated conditions are shown in Fig. 3b. Therefore, when porosity of the studied rocks increases the ultrasonic wave velocity decreases. Also, the presence of water in the peridotites increases the sound velocities independently of effective porosity values.

Correlations between dry unit weight with dry and saturated P and S wave velocity are presented in Fig. 4a and b, respectively, and determination coefficient was found between 0.74 and 0.85. These relations are directly linear, therefore when unit weight of the studied rocks increases the P and S wave velocity increase.

Correlation between dry V_P and saturated V_P is presented in Fig. 5a. This relation is direct linear with coefficient of determination $R^2=0.91$.Direct linear correlation between dry and saturated V_S with coefficient of determination $R^2=0.93$ is shown in Fig. 5b. Other correlations between V_P and V_S in dry and saturated conditions are presented in Fig. 5c and d.

Dynamic elastic constants

Elastic characteristics of rocks are measured from dynamic and static procedures [36]. In the static or destructive method, uniaxial stresses are applied on the core samples until failure occurs. The static elastic properties and uniaxial compressive strength of the rocks are obtained by studying the stress-deformation curves (estimated in next section, [37]). In dynamic or non-destructive method, elastic constants were calculated by using obtained results of compressional and shear ultrasonic wave velocities (V_P and V_S) [38]. In this research, dynamic elastic constants including bulk modulus (K), shear modulus (G), Poisson's ratio (ν) and elasticity modulus (E) are calculated by the following equations [35]:

$$K = \rho_b\left(V_P^2 - \frac{4}{3}V_S^2\right) \quad (5)$$

$$G = \rho_b V_S^2 \quad (6)$$

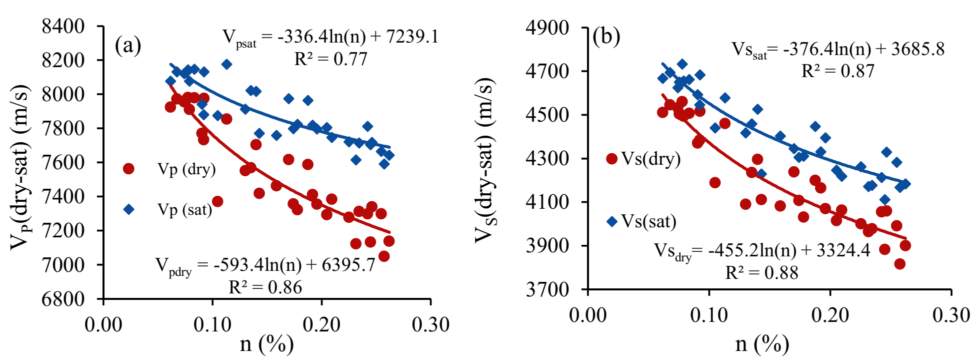

Fig. 3 Correlations between porosity and **a** dry and saturated P-wave velocity and **b** dry and saturated S-wave velocity

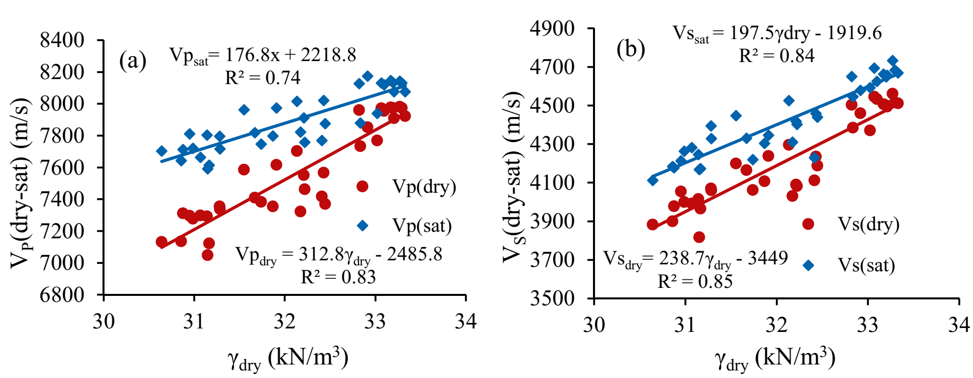

Fig. 4 Correlations between dry unit weight and **a** dry and saturated P-wave velocity and **b** dry and saturated S-wave velocity

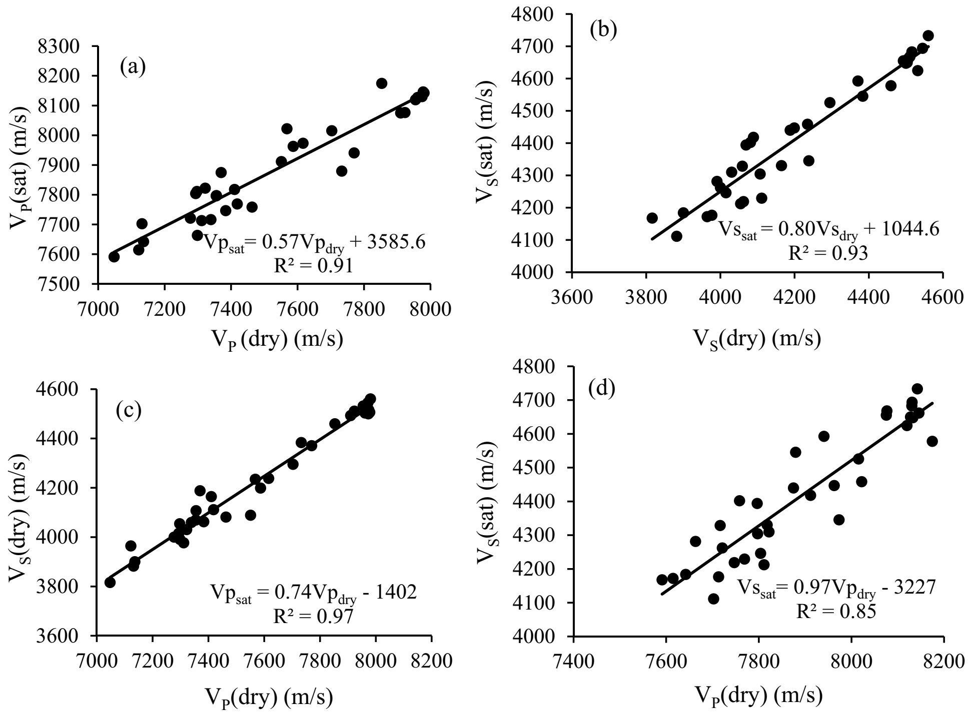

Fig. 5 Correlations between **a** dry and saturated P-wave velocity, **b** dry and saturated S-wave velocity, **c** dry P-wave velocity and dry S-wave velocity and **d** dry P-wave velocity and saturated S-wave velocity

$$\nu = \frac{(V_P^2 - 2V_S^2)}{2(V_P^2 - 2V_S^2)} \tag{7}$$

$$E = 2G(1 + \nu) \tag{8}$$

where ρ is the bulk density, V_P and V_S are the compressional and shear ultrasonic wave velocities of the samples, respectively. The minimum, the maximum, the average value and the standard deviation of the dynamic elastic constants are listed in Table 3.

In order to determine the relationships between dynamic elastic constants in dry and saturated conditions, statistical correlations were performed by simple regression analysis. Relationships between dry and saturated bulk modulus, dry and saturated shear modulus and dry and saturated elasticity modulus are illustrated in Fig. 6a, b and d, respectively. The relations are linear and the determination coefficients range between 0.67 and 0.97. While relationships between dry and saturated Poisson's ratio is direct power relation with low determination coefficient equal to $R^2 = 0.55$ (Fig. 6c). Because the Poisson's ratio has small values (lower than 0.5) in comparison to other dynamic properties, the change of its determination coefficient is very sensitive, and this causes to decrease of the coefficient. Also, inhomogeneity or laboratory test errors can sometimes be led to decrease in coefficient of determination.

Strength and deformation parameters

In this research for determining strength and deformation of the studied rocks, some mechanical properties including uniaxial compressive strength (UCS), elasticity modulus (E) and Brazilian tensile strength (BTS) were performed

Table 3 Basic descriptive statistical analysis of the dynamic elastic constants for the peridotite rocks

Property	Minimum value	Maximum value	Mean value	Standard deviation
Dry bulk modulus, $K_{(dry)}$ (GPa)	92.78	121.41	107.39	9.38
Saturated bulk modulus, $K_{(sat)}$ (GPa)	106.52	127.98	116.45	5.71
Dry shear modulus, $G_{(dry)}$ (GPa)	45.37	69.19	57.25	7.69
Saturated shear modulus, $G_{(sat)}$ (GPa)	51.78	74.53	62.95	7.03
Dry Poisson's ratio, $\nu_{(dry)}$	0.26	0.29	0.27	0.01
Saturated Poisson's ratio, $\nu_{(sat)}$	0.24	0.30	0.27	0.02
Dry elasticity modulus, $E_{(dry)}$ (GPa)	117.28	174.03	146.02	19.32
Saturated elasticity modulus, $E_{(sat)}$ (GPa)	134.72	185.55	159.63	16.83

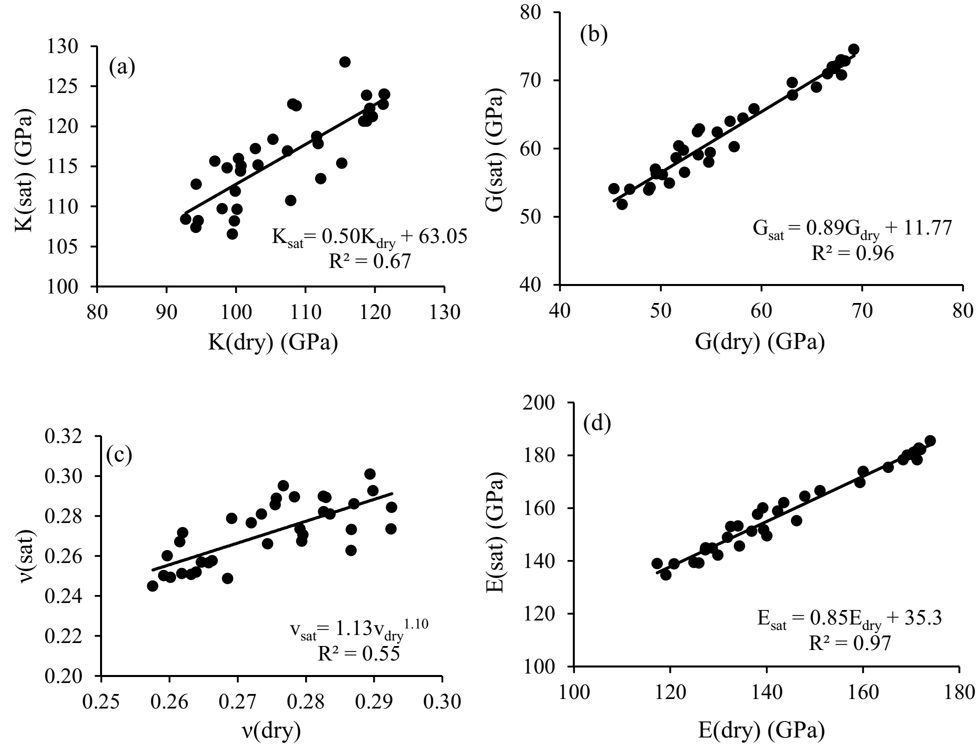

Fig. 6 Correlations between **a** dry and saturated bulk modulus, **b** dry and saturated shear modulus, **c** dry and saturated Poisson's ratio and **d** dry and saturated elasticity modulus

in saturated conditions, while the same property values in dry conditions were obtained by Diamantis [26, 27].

The UCS tests were carried out using a servo-controlled hydraulic testing machine in accordance with ASTM [39]. The elasticity modulus was derived from the slope of the stress–strain curves at the 50% of the maximum UCS. The prepared core specimens with average diameter of 54 mm (NX, range from 53 to 55 mm) and a length to diameter ratio in range of 2–2.5 [40] were used for determining UCS of the studied rocks. The UCS values were ranged from 65.21 to 241.56 MPa and 52.32 to 240.90 MPa for dry and saturated conditions, respectively, exhibiting a great fluctuation. This great difference may be due to the internal discontinuities, macroscopically undetected and/or the different degrees of serpentinization and/or petrographic variety and/or the structural complexity of peridotites.

Therefore, the uniaxial compressive strength of the studied rocks decreased averagely 8.19% after saturation. Average values of UCS were obtained equal to 142.07 and 132.53 MPa for dry and saturated conditions, respectively. Therefore, based on ISRM [29], the tested samples were classified as high to extremely high strength rocks in both dry and saturated conditions. The elasticity modulus values were 26.40 to 69.34 GPa and 21.27 to 68.75 GPa, in dry and saturated conditions, respectively. So, the elasticity modulus of the studied rocks decreased averagely 8.43% after saturation. This means that the presence of water in the rock structure reduces its modulus of elasticity.

The Brazilian tensile strength test as simple indirect method for determining tensile strength of rocks were carried out on prepared core specimens with thickness to diameter ratios 0.5 based on ISRM [29]. Brazilian tensile strength was determined by the following equation:

$$\mathrm{BTS} = \frac{2P}{\pi D t} \tag{9}$$

where, P is the maximum load, D is the diameter, and t is the thickness of the specimen.

The BTS values were ranged from 11.76 to 24.93 MPa and 9.74 to 24.06 MPa in dry and saturated conditions, respectively. Average values of BTS were obtained equal to 18.67 and 16.64 MPa in dry and saturated conditions, respectively. Therefore, the Brazilian tensile strength of the studied rocks was reduced averagely 11.71% after saturation. Results of mechanical properties testing indicated that after saturation average value of BTS decrease (reduce = 11.71%) more than UCS (reduce = 8.19%). Therefore, saturation affected more tensile strength of studied rocks than compressive strength. Similar results were found by [41–45] for several rocks.

Obtained values of mechanical properties including uniaxial compressive strength, elasticity modulus and Brazilian tensile strength for the studied rocks in dry and saturated conditions are listed in Table 4.

Table 4 Values of the mechanical properties for the studied peridotite rocks in dry [26, 27] and saturated conditions

Sample	Strength parameters					
	UCS (MPa)		E (GPa)		BTS (MPa)	
	Dry	Sat	Dry	Sat	Dry	Sat
P1	112.37	91.26	43.47	38.85	16.54	14.25
P2	131.36	130.14	37.09	34.46	19.06	18.03
P3	96.23	80.39	38.90	35.51	16.76	14.41
P4	71.12	60.35	27.08	23.97	15.17	12.87
P5	122.85	107.25	35.62	33.25	18.03	14.94
P6	136.34	130.67	36.04	33.84	18.60	15.71
P7	65.21	52.32	26.50	21.27	16.31	13.1
P8	112.36	102.66	36.31	34.26	16.74	15.3
P9	79.31	58.33	29.58	22.74	13.59	10.46
P10	172.35	168.49	60.07	55.72	21.99	19.45
P11	135.61	99.35	41.02	37.06	11.97	9.97
P12	74.44	65.46	29.34	25.80	11.76	9.74
P13	84.98	69.99	31.29	26.11	12.49	10.42
P14	188.82	187.94	63.13	62.06	23.09	22.67
P15	179.61	176.43	64.50	62.94	20.46	19.84
P16	197.44	184.22	63.93	60.64	21.36	19.91
P17	105.43	102.35	42.48	40.89	16.44	14.95
P18	185.60	178.18	49.56	47.58	24.79	22.67
P19	148.89	145.18	43.93	41.76	17.32	14.89
P20	178.15	171.02	49.97	42.97	19.28	18.5
P21	185.17	167.76	54.38	48.27	22.50	21.75
P22	156.06	136.31	38.45	31.58	16.56	12.21
P23	241.56	240.90	69.34	68.75	24.93	24.06
P24	189.14	181.57	63.88	59.35	24.64	23.95
P25	201.81	196.88	61.18	58.68	24.35	22.97
P26	198.71	194.77	65.03	60.74	22.33	21.89
P27	205.39	204.71	66.28	66.06	23.55	23.17
P28	138.64	133.10	42.49	38.79	13.67	12.72
P29	121.34	116.49	39.75	36.16	13.97	12.25
P30	131.60	126.34	26.40	25.74	15.18	14.57
P31	107.75	102.02	34.65	31.80	20.69	16.59
P32	183.47	176.13	54.37	52.19	22.50	21.76
P33	117.41	100.77	32.27	30.70	19.67	15.18
P34	92.35	84.33	29.12	24.59	19.55	14.85
P35	123.58	114.64	32.61	28.25	17.75	12.46

Effect of porosity on strength and deformation

Some researchers attempted to estimate indirect of the UCS of different rocks by using porosity values and developed empirical equations [23, 46–50]. In this regard, Harthi [51] studied the porosity of igneous rock and linear regression equations were presented for predicting uniaxial compressive strength: UCS = 274–8.51n for $n < 20\%$ and UCS = 104–1.01n for $n > 20\%$. [52] investigated the influence of apparent porosity on uniaxial compressive strength of some volcanic rocks.

In this study, correlations between porosity and uniaxial compressive strength, elasticity modulus and Brazilian tensile strength in dry and saturated conditions were found by simple regression analysis and graphs are illustrated in Fig. 7a to c, respectively. Reverse logarithmic equations with determination coefficient in range of 0.69–0.80 was found. Based on the results it's obvious when the porosity decreases, the UCS, E and BTS increase.

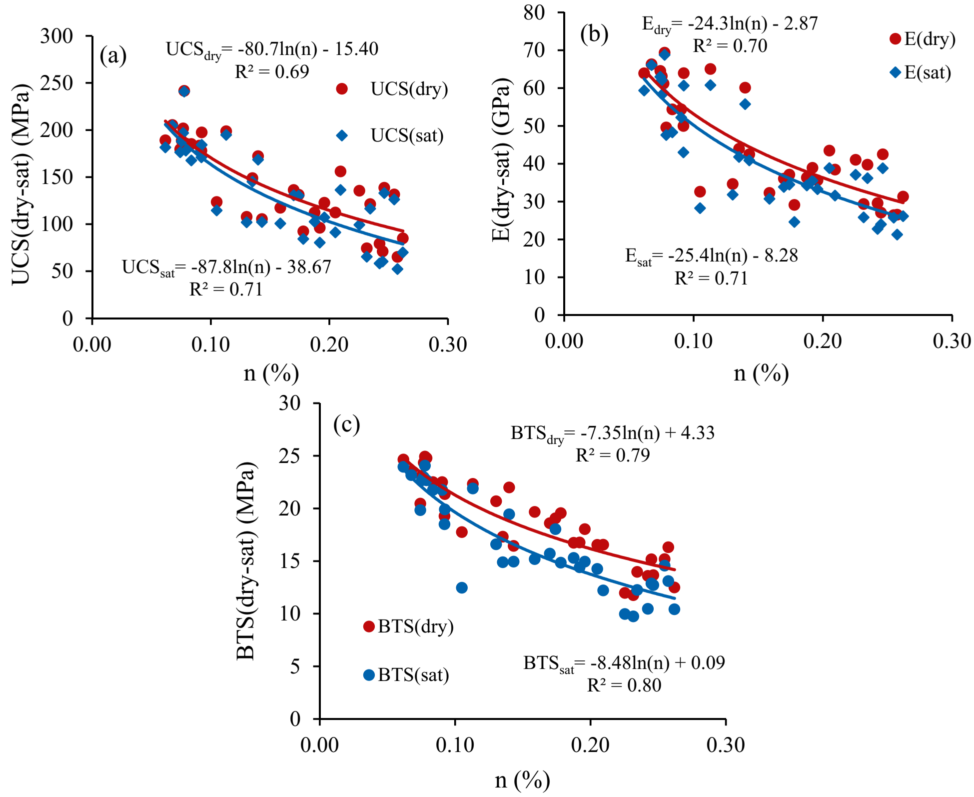

Fig. 7 Correlations between porosity and **a** dry and saturated uniaxial compressive strength, **b** dry and saturated elasticity modulus and **c** dry and saturated Brazilian tensile strength

Effect of dry unit weight on strength and deformation

Some researcher assessed the effect of dry unit weight on uniaxial compressive strength of rocks (e.g. [34, 53–57]). Plots of correlations between dry unit weight with dry and saturated UCS are illustrated in Fig. 8a. The linear equations are obtained with medium coefficient of determination $R^2=0.68$ and $R^2=0.70$ for dry and saturated conditions, respectively. The linear correlations presents relationships between dry unit weight with dry and saturated elasticity modulus with coefficient of determination equal to $R^2=0.64$ for dry and saturated conditions, respectively (Fig. 8b). Based on the trend lines of Fig. 8c, the relation between dry unit weight and BTS in dry conditions presents little better correlation ($R^2=0.80$) than saturated stages ($R^2=0.77$). As a general conclusion, when dry unit weight increases, the UCS, E and BTS increase.

Relationships between wave velocity, strength and deformation

Many researchers studied relationships between wave velocity and uniaxial compressive strength [23, 58–61], tensile strength [62, 63] and elasticity modulus [64–67] for several rocks.

The relationships between dry P-wave velocity with uniaxial compressive strength, elasticity modulus and Brazilian tensile strength in dry and saturated conditions are presented in Fig. 9a to c, respectively. Based on the results, these relations are directly linear and determination coefficient obtained in range of 0.77–0.85. In this research, beside correlations of V_P, the relationships between dry S-wave velocity with UCS, E and BTS in dry and saturated conditions are analyzed by regression technique that is illustrated in Fig. 9d to f. Results are close to V_P correlations and direct linear relations with coefficient of determination in range of 0.73–0.83 were obtained.

Relationships between strength and deformation parameters

In recent years, the relationships between dry and saturated UCS for various rocks were studied by many researchers and experimental equations have been concluded (e.g. [7–11, 68, 69]). Based on the graph of Fig. 10a, direct linear correlation is established between dry and saturated UCS and very high coefficient of determination ($R^2=0.98$) was found. Many studies, attempted to correlate the E_{dry} with E_{sat} [42–44, 70–72]. In this research, the linear equation presents very strong correlation with coefficient of determination $R^2=0.99$ between dry and saturated elasticity modulus (Fig. 10b). Relationships between Brazilian tensile strengths in dry and saturated conditions are illustrated in Fig. 10c. There is a

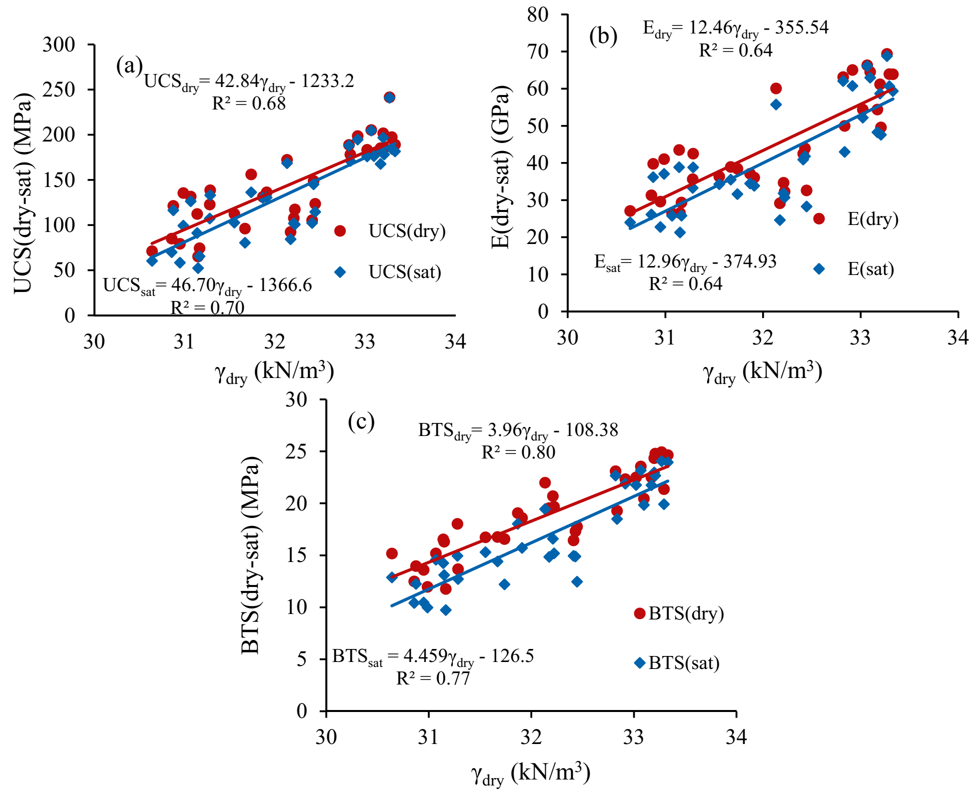

Fig. 8 Correlations between dry unit weight and **a** dry and saturated uniaxial compressive strength, **b** dry and saturated elasticity modulus and **c** dry and saturated Brazilian tensile strength

direct linear relation with good coefficient of determination equal to $R^2 = 0.92$.

Many researchers have investigated the relations between strength and deformation characteristics for several rocks. In this research, for assessing the relationships between mechanical properties including UCS, E and BTS in dry and saturated conditions some correlations were performed. Correlations between dry UCS and E in dry and saturated conditions with acceptable coefficient of determination ($R^2 = 0.83$) is shown in Fig. 11a. Direct linear correlations between dry BTS with dry and saturated values of UCS are shown in Fig. 11b. Medium coefficient of determination equal to 0.63 and 0.66 were obtained for dry and saturated conditions, respectively. Correlations between dry values of BTS with dry and saturated elasticity modulus with low coefficient of determination (0.58 and 0.59) are illustrated in Fig. 11c.

Summary and conclusions

In this research, the effect of water saturation on the physical properties, wave velocities, strength and deformation of 35 samples of peridotite rocks were investigated. 35 samples of peridotite rocks, taken from the same places in central Greece as they reported in Diamantis [26, 27], were tested in saturated conditions and the values of static and dynamic tests were determined.

Peridotite rock samples were collected from two regions of the central Greece including eastern-southeastern part of Kallidromo Mt. and western part of Othrys Mt. The investigated samples are peridotites which are mainly medium-grained, homogeneous, isotropic rocks with granular or porphyritic structure. Results of tests on physical properties show the porosity of the studied rocks is classified as very low while the unit weight as very high. Obtained values of the ultrasonic wave velocities show P and S waves were increased after saturation. Regression analyses show reverse logarithmic and direct linear relations between porosity and unit weight with P and S wave velocities in dry and saturated conditions, respectively. According to the results, the mechanical properties namely UCS, *E*, and BTS were decreased after saturation. Reverse logarithmic equations was found between porosity with UCS, E, and BTS. Direct linear correlations among dry unit weight with UCS, E, and BTS indicated that when γ_{dry} increases, the mechanical properties are increased. The relationships between dry P and S wave velocities with UCS, E and BTS in dry and saturated conditions were assessed and R^2 obtained in range of 0.73–0.85. Linear correlations between dry and saturated values of UCS, E

Fig. 9 Correlations between dry P-wave velocity and **a** dry and saturated uniaxial compressive strength, **b** dry and saturated elasticity modulus, **c** dry and saturated Brazilian tensile strength and correlation between dry S-wave velocity and **d** dry and saturated uniaxial compressive strength, **e** dry and saturated elasticity modulus and **f** dry and saturated Brazilian tensile strength

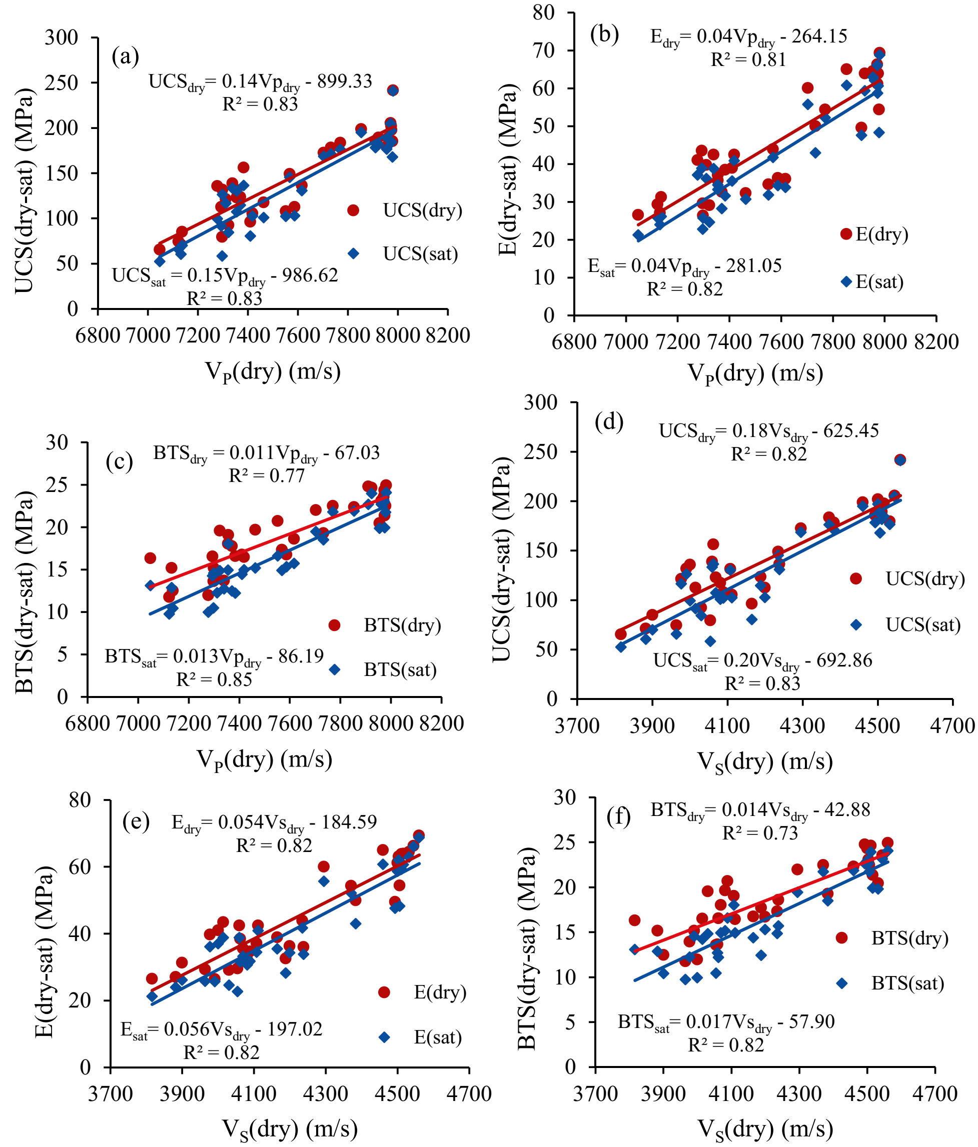

and BTS were performed and regression equations with strong coefficient of determination were obtained. Results of this research in the form of some experimental equations for determining static and dynamic properties of peridotite rocks in dry and saturated conditions with coefficient of determination in range of 0.55–1 are presented. To sum up, the above-mentioned results revealed change in the physical, dynamic, and mechanical properties with the presence of water. So, the presence of water or moisture can be led to decrease of rock engineering quality when they are used in engineering projects.

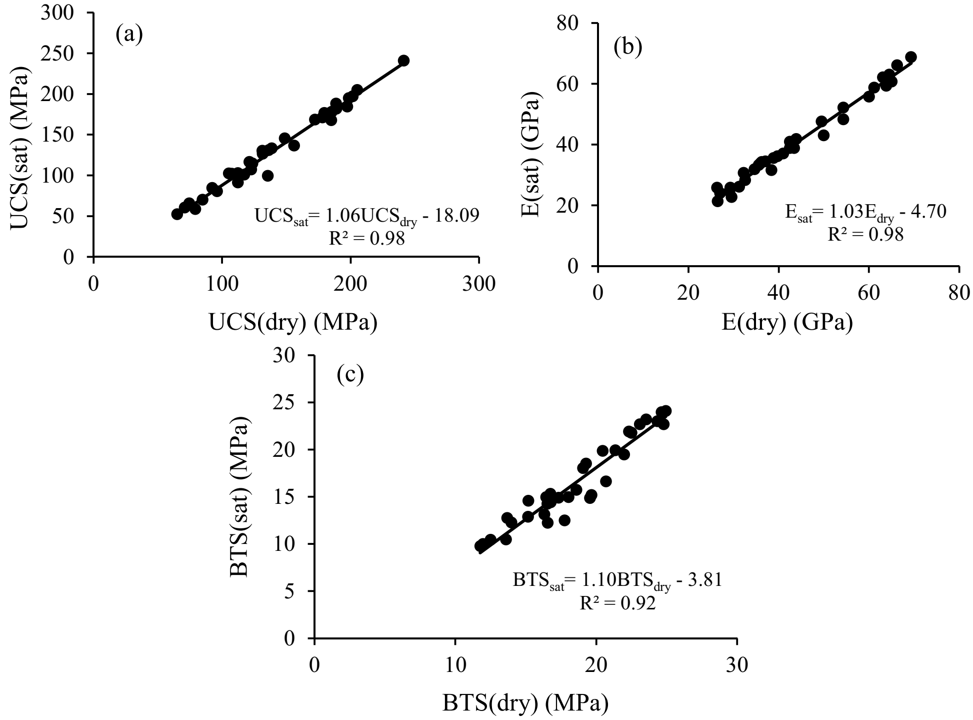

Fig. 10 Correlations between **a** dry and saturated uniaxial compressive strength, **b** dry and saturated elasticity modulus and **c** dry and saturated Brazilian tensile strength

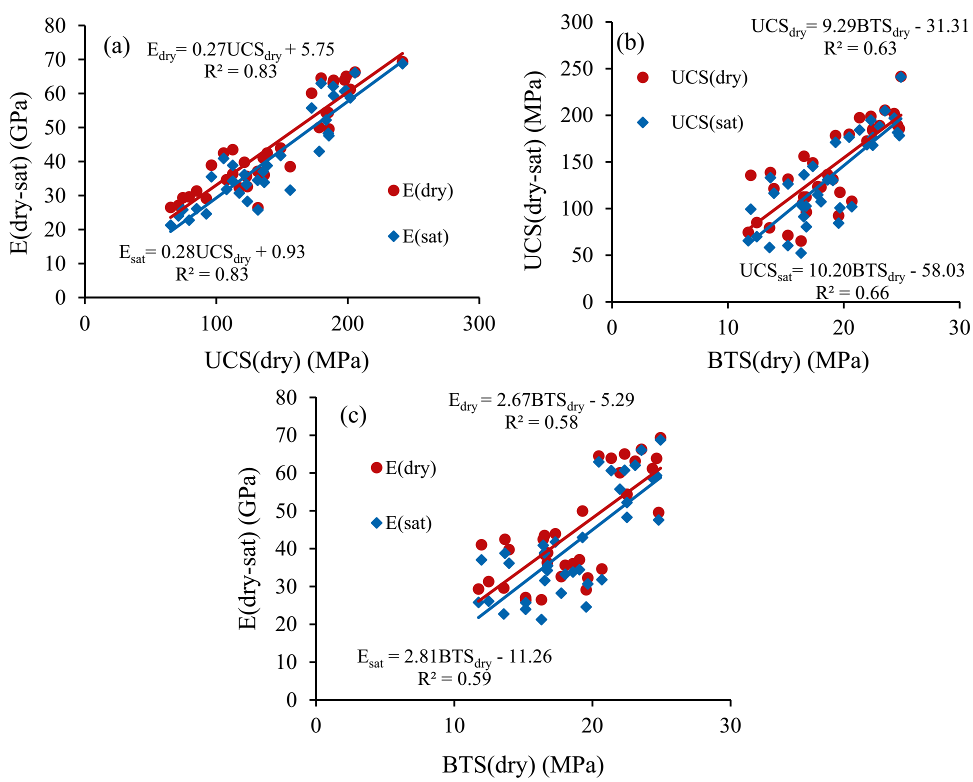

Fig. 11 Correlations between **a** dry uniaxial compressive strength and dry and saturated elasticity modulus, **b** dry Brazilian tensile strength and dry and saturated uniaxial compressive strength and **c** dry Brazilian tensile strength and dry and saturated elasticity modulus

Author contributions All authors contributed to the study conception and design. Material preparation, data collection and analysis were performed by KD. The first draft of the manuscript was written by KD and all authors commented on previous versions of the manuscript. All authors read and approved the final manuscript.

Funding The authors declare that no funds, grants, or other support were received during the preparation of this manuscript.

Declarations

Conflict of interest The authors have no competing interests to declare that are relevant to the content of this article.

Ethical approval This article does not contain any studies with human participants or animals performed by any of the authors.

Informed consent For this type of study, formal consent is not required.

References

1. Daraei A, Zare S (2018) Determination of critical saturation degree in rocks based on maximum loss of uniaxial compression strength and deformation modulus. Geomech Geophys Geo-energ Geo-resour 4:343–353
2. Khajevand (2021) Evaluating the influence of petrographic and textural characteristics on geotechnical properties of some carbonate rock samples by empirical equations. Innov Infrastruct Solut 6(6):113. https://doi.org/10.1007/s41062-021-00498-w
3. Song K, Wang F, Yi Q, Lu S (2018) Landslide deformation behavior influenced by water level fluctuations of the three Gorges Reservoir (China). Eng Geol 247:58–68
4. Lafrance N, Auvray C, Souley M, Labiouse V (2016) Impact of weathering on macromechanical properties of chalk: local pillar-scale study of two underground quarries in the Paris Basin. Eng Geol 213:107–119
5. Dang W, Wu W, Konietzky H, Qian J (2019) Effect of shear-induced aperture evolution on fluid flow in rock fractures. Comput Geotech. https://doi.org/10.1016/j.compgeo.2019.103152
6. Bajni G, Apuani T, Beretta GP (2019) Hydro-geotechnical modelling of subsidence in the Como urban area. Eng Geol. https://doi.org/10.1016/j.enggeo.2019.105144
7. Liu H, Zhu W, Yu Y, Xu T, Li R, Liu X (2020) Effect of water imbibition on uniaxial compression strength of sandstone. Int J Rock Mech Min Sci 127:104200. https://doi.org/10.1016/j.ijrmms.2019.104200
8. Luo Y (2020) Influence of water on mechanical behavior of surrounding rock in hard-rock tunnels: An experimental simulation. Eng Geol 277:105816. https://doi.org/10.1016/j.enggeo.2020.105816
9. Tang SB, Yu CY, Heap MJ, Chen PZ, Ren YG (2018) The influence of water saturation on the short and long-term mechanical behavior of red sandstone. Rock Mech and Rock Eng 51:2669–2687
10. Yu CY, Tang SB, Tang CA, Duan D, Zhang YJ, Liang ZZ, Ma K, Ma TH (2019) The effect of water on the creep behavior of red sandstone. Eng Geol 253:64–74
11. Zhao K, Yang D, Zeng P, Huang Z, Wu W, Li B, Teng T (2021) Effect of water content on the failure pattern and acoustic emission characteristics of red sandstone. Int J Rock Mech Min Sci 142:104709. https://doi.org/10.1016/j.ijrmms.2021.104709
12. Song C, Feng G, Bai J, Cui J, Wang K, Shi X, Qian R (2023) Progressive failure characteristics and water-induced deterioration mechanism of fissured sandstone under water–rock interaction. The App Frac Mech 128:104151
13. Ping S, Wang F, Wang D, Li S, Yuan Y, Feng G, Shang S (2023) Multi-scale deterioration mechanism of shear strength of gypsum-bearing mudstone induced by water-rock reactions. Eng Geol 323:107224
14. Yu H, Liu Z, Zhang Y, Luo T, Tang Y, Zhang Q, Wang Y (2023) The disintegration mechanism analysis of soft rock due to water intrusion based on discrete element method. Comp Geosc 171:105289
15. Zhu J, Deng J, Chen F, Wang F (2022) Failure analysis of water-bearing rock under direct tension using acoustic emission. Eng Geol 299:106541
16. Liu CD, Cheng Y, Jiao YY, Zhang GH, Zhang WS, Ou GZ, Tan F (2021) Experimental study on the effect of water on mechanical properties of swelling mudstone. Eng Geol 295:106448
17. Katsikatsos G, Migiros G, Triantaphyllis M, Mettos A (1986) Geological structure of internal Hellenides (E. Thessaly-SW Macedonia. Euboea-Attica-Northern Cyclades islands and Lesvos). I.G.M.E. Geol and Geoph Res Special Issue 191–212.
18. Guha Roy D, Singh TN, Kodikara J, Das R (2017) Effect of water saturation on the fracture and mechanical properties of sedimentary rocks. Rock Mech Rock Eng 50:2585–2600
19. Kou M, Liu X, Tang S, Wang Y (2019) 3-D X-ray computed tomography on failure characteristics of rock like materials under coupled hydro-mechanical loading. Theor Appl Fract Mech. https://doi.org/10.1016/j.tafmec.2019.102396
20. Kou M, Liu X, Wang Y (2020) Study on rock fracture behavior under hydromechanical loading by 3-D digital reconstruction. Struct Eng Mech 74:283–296
21. Zhou Z, Cai X, Ma D, Cao W, Chen L, Zhou J (2018) Effects of water content on fracture and mechanical behavior of sandstone with a low clay mineral content. Eng Fract Mech 193:47–65
22. Diamantis K (2019) Estimation of tensile strength of ultramafic rocks using indirect approaches. Geom and Eng 17(3):261–270. https://doi.org/10.12989/gae.2019.17.3.261
23. Diamantis K, Gartzos E, Migiros G (2009) Study on uniaxial compressive strength point load strength index, dynamic and physical properties of serpentinites from Central Greece: test results and empirical relations. Eng Geol 108:199–207
24. Khajevand R, Fereidooni D (2019) Utilization of the point load and block punch strengths to predict the mechanical properties of several rock samples using regression analysis methods. Innov Infrastruct Solut. https://doi.org/10.1007/s41062-019-0201-8
25. Moussas V, Diamantis K (2021) Predicting uniaxial compressive strength of serpentinites through physical, dynamic and mechanical properties using neural networks. J Rock Mech Geotech Eng 13:167–175
26. Diamantis K (2010) Engineering geological properties of the ultrabasic rocks in Othrys and Kallidromo mountains (central Greece). Phd Thesis, Athens, p 386. Agricultural University of Athens.
27. Diamantis K, Bellas S, Migiros G, Gartzos E (2011) Correlating wave velocities with physical, mechanical properties and petrographic characteristics of peridotites from the central Greece. Geotech Geol Eng 29:1049–1062
28. Mountrakis D, Sapountzis E, Kilias A, Eleftheriadis G, Christofides G (1983) Paleogeographic conditions in the western Pelagonian margin in Greece during the initial rifting of the continental area. Canad Jou Ear Sc 20:1673–1681
29. ISRM (International Society of Rock Mechanics) (2007) The blue book: the complete ISRM suggested methods for rock characterization, testing and monitoring: 1974–2006. In: Ulusay R, Hudson JA (eds) Kazan Offset Press. Ankara
30. Goodman RE (1989) Introduction to rock mechanics, 2nd edn. John Wiley & Sons Publication, New York
31. IAEG (1979) Classification of rocks and soils for engineering geological mapping, report by the IAEG commission on engineering geological mapping. Bulletin of IAEG 24:235–274
32. Irfan TY, Dearman WR (1978) The engineering petrography of a weathered granite in Cornwall, England. Q J Eng Geol 11:233–244

33. Kurtulus C, Bozkurt A, Endes H (2011) Physical and mechanical properties of serpentinized ultrabasic rocks in NW Turkey. Pure Appl Geophys 169(7):1205–1215
34. Tuğrul A, Zarif IH (1999) Correlation of mineralogical and textural, characteristics with engineering properties of selected granitic rocks from Turkey. EngGeol 51:303–317
35. ASTM D2845-D2895 (1996) Standard test method for laboratory determination of pulse velocities and ultrasonic elastic constants of rock (withdrawn 2017). ASTM International, West Conshohocken
36. Al-Shayea NA (2004) Effects of testing methods and conditions on the elastic properties of limestone rock. Eng Geol 74(1):139–156
37. Jaeger JC, Cook NGW, Zimmerman RW (2007) Fundamentals of rock mechanics, 4th edn. Blackwell Publishing, Oxford
38. Najibi AR, Ghafoori M, Lashkaripour GR (2015) Empirical relations between strength and static and dynamic elastic properties of Asmari and Sarvak limestones, two main oil reservoirs in Iran. J Pet Sci Eng 126:78–82
39. ASTM D2938 (1995) Standard test method of unconfined compressive strength of intact rock core specimens, American Society for Testing and Materials (reapproved 2002)
40. ASTM D4543 (2001) Standard practices for preparing rock core specimens and determining dimensional and shape tolerances. American Society for Testing and Materials, West Conshohocken
41. Erguler ZA, Ulusay R (2009) Water-induced variations in mechanical properties of clay-bearing rocks. Int J Rock Mech Min Sci 46:355–370
42. Karakul H, Ulusay R (2013) Empirical correlations for predicting strength properties of rocks from P-wave velocity under different degrees of saturation. Rock Mech Rock Eng 46(5):981–999
43. Vásárhelyi B (2005) Statistical analysis of the influence of water content on the strength of the miocene limestone. Rock Mech Rock Eng 38:69–76
44. Vásárhelyi B, Davarpanah M (2018) Influence of the water content on the mechanical parameters of the intact rock and rock mass. Period Polytech Civ Eng 62(4):1060–1066
45. Wong LN, Jong MC (2014) Water saturation effects on the Brazilian tensile strength of gypsum and assessment of cracking processes using high-speed video. Rock Mech Rock Eng 47:1103–1115
46. Aladejare AE (2020) Evaluation of empirical estimation of uniaxial compressive strength of rock using measurements from index and physical tests. J Rock Mech Geotech Eng 12(2):256–268
47. Chen X, Schmitt DR, Kessler JA, Evans J, Kofman R (2015) Empirical relations between ultrasonic P wave velocity, porosity and uniaxial compressive strength. CSEG Rec 40(05):24–29
48. Horsrud P (2001) Estimating mechanical properties of shale from empirical correlations. SPE Drill Complet 16:68–73
49. Mishra DA, Basu A (2013) Estimation of uniaxial compressive strength of rock materials by index tests using regression analysis and fuzzy inference system. Eng Geol 160:54–68
50. Tuğrul A (2004) The effect of weathering on pore geometry and compressive strength of selected rock types from Turkey. Eng Geol 75:215–227
51. Harthi AA, Al-Amri RM, Shehata WM (1999) The porosity and engineering properties of vesicular basalt in Saudi Arabia. Eng Geol 54(3–4):313–320
52. Karaman K, Kesimal A (2015) Evaluation of the influence of porosity on the engineering properties of volcanic rocks from the Eastern black sea region: NE Turkey. Arab J Geosci 8:557–564
53. Deere DU, Miller RP (1966) Engineering classification and index properties for intact rocks. Tech Rep Air Force Weapons Lab, New Mexico, no AFNL-TR, 65–116
54. Gupta V (2009) Non-destructive testing of some higher Himalayan rocks in the Satluj Valley. Bull EngGeol Environ 68:409–416
55. Hebib R, Belhai D, Alloul B (2017) Estimation of uniaxial compressive strength of North Algeria sedimentary rocks using density, porosity, and Schmidt hardness. Arab J Geosci 10. https://doi.org/10.1007/s12517-017-3144-4
56. Shalabi FI, Cording EJ, Al-Hattamleh OH (2007) Estimation of rock engineering properties using hardness tests. Eng Geol 90:138–147
57. Tuğrul A, Gürpinar O (1997) A proposed weathering classification for basalts and their engineering properties (Turkey). Bull Eng Geol Environ 55(1):139–149
58. Cobanoglu I˙, Celik SB, (2008) Estimation of uniaxial compressive strength from point load strength, Schmidt hardness and P-wave velocity. Bull Eng Geol Environ 67(4):491–498
59. Khandelwal M (2013) Correlating P-wave velocity with the physico-mechanical properties of different rocks. Pure Appl Geophys 170(4):507–514
60. Sarkar K, Vishal V, Singh TN (2012) An empirical correlation of index geo-mechanical parameters with the compressional wave velocity. Geotech Geol Eng 30(2):469–479
61. Sharma PK, Singh TN (2008) A correlation between P-wave velocity, impact strength index, slake durability index and uniaxial compressive strength. Bull Eng Geol Environ 67:17–22
62. Kurtulus C, Sertcelik F, Sertcelik I (2015) Correlating physico-mechanical properties of intact rocks with P-wave velocity. Acta Geod Geophys 51:571–582
63. Vasconcelos G, Lourenço PB, Alves CAS, Pamplona J (2008) Ultrasonic evaluation of the physical and mechanical properties of granites. Ultrasonics 48(5):453–466
64. Altindag R (2012) Correlation between P-wave velocity and some mechanical properties for sedimentary rocks. J South Afr Inst Min Metall 11(3):229–237
65. Khandelwal M, Singh TN (2009) Correlating static properties of coal measures rocks with P-wave velocity. Int J Coal Geol 79:55–60
66. Wen L, Luo ZQ, Yang SJ, Qin YG, Wang W (2019) Correlation of geo-mechanics parameters with uniaxial compressive strength and P-wave velocity on dolomitic limestone using a statistical method. Geotech Geo Eng 37(2):1079–1094
67. Yasar E, Erdogan Y (2004) Correlating sound velocity with the density, compressive strength and Young's modulus of carbonate rocks. Int J Rock Mech Mining Sci 41:871–875
68. Wong LNY, Maruvanchery V, Liu G (2016) Water effects on rock strength and stiffness degradation. Acta Geotech 11:713–737
69. Zhou Z, Cai X, Cao W, Li X, Xiong C (2016) Influence of water content on mechanical properties of rock in both saturation and drying processes. Rock Mech Rock Eng 49:3009–3025
70. Ván P, Vásárhelyi B (2014) Sensitivity analysis of GSI based mechanical parameters of the rock mass. Perio Polytec Civil Eng 58(4):379–386
71. Vásárhelyi B (2003) Some observation regarding the strength and deformability of sandstones in case of dry and saturated conditions. Bull Eng Geol Environ 62:245–249
72. Yilmaz I (2010) Influence of water content on the strength and deformability of gypsum. Int J Rock Mech Min Sci 47:42–347